RESEARCH PAPER

Numerical Modelling and Industrial Verification of Ethylene Dichloride Cracking Furnace

Afshin Fahiminezhad, Seyed Mohsen Peyghambarzadeh*, Mohsen Rezaeimanesh

Department of Chemical Engineering, Mahshahr Branch, Islamic Azad University, Mahshahr, Iran

Abstract

In this paper, the radiation section of ethylene dichloride (EDC) cracking furnace, considering the chemical reaction, was numerically modelled using computational fluid dynamics (CFD). This study investigated the influence of some parameters such as mass flow rate, the inlet temperature of fluid into the radiation section, and heat flux on the conversion and changes in velocity, pressure, and temperature of the fluid along the coil passes, as well as the outlet stream of the coil. Then, the modelling results were compared with a series of industrial data of an industrial EDC cracking furnace. The results showed that considering the variable heat flux boundary condition is more compatible with the industrial data rather than the constant heat flux boundary condition. Increasing the feed inlet temperature to the furnace, increased the EDC conversion due to the endothermic nature of the thermal cracking reaction. Furthermore, reducing the inlet mass flow rate led to a significant increase in the conversion, temperature, and mass fraction of the products due to an increase in residence time.

Introduction

Generally, the simulation of industrial combustion and chemical reaction involves the solution of turbulent flows along with heat transfer, mass transfer, and chemical reaction. In the last two decades, there has been a lot of progress in applications of fluid dynamics calculations in industrial combustion. Nowadays, the CFD tool is used to analyze a variety of problems such as boilers, furnaces, fluidized beds, combustion chambers of gas turbines, and many other applications. The fluid dynamics calculations are a theoretical solution for the assessment and prediction of the performance of systems that involve fluid flow, energy transfer, and related phenomena such as combustion and chemical reactions. The CFD codes solve the equations of mass, energy, and momentum conservation on a domain that is specified by the user. This technique is very robust and includes a wide range of industrial applications.

Nowadays, CFD modelling has wide applications in advanced industries and optimization of industrial processes. In the last few years, an increase in the power of computers has given the ability to engineers to accurately modelling the multiphase flows in very complex geometry. As a result of these advances, the application of CFD in the industrial processes is increasing rapidly. One of the most important CFD applications is modelling of industrial combustion. The combustion is one of the most complicated transfer phenomena. In modelling of this phenomenon, the influences of reactive flows, fluid dynamics, reaction chemistry, reaction kinetics, radiation, and how these phenomena interact with each other should be considered.

Hu et al. [1] studied the simulation of complete convective heat transfer in the furnace chamber and its coils. They simulated the industrial furnace of ethylene cracking with CFD

---

* Corresponding author:
Email: m.peyghambarzadeh@mhriau.ac.ir (S. M. Peyghambarzadeh)

method using a two-stage combination of steam and feed. To simulate the ethylene cracking furnace, they employed the convective heat transfer inside the furnace chamber, κ-ε standard method, and discrete-oriented (DO) radiative model, respectively, in describing the turbulence characteristics and the radiative heat transfer. They also used the RNG κ-ε method and volume of fluid (VOF) for turbulent flow and two-phase vapor-liquid flow in the simulation of momentum transfer inside the coil. Finally, they compared the agreement of the obtained results with the industrial data which yielded good results in their comparison.

Li et al. [2] analyzed the cause of the leak in the convection section of the ethylene cracking furnace. To study the cause of failure, the failed tubes were investigated with macro inspections, chemical composition analysis, metallographic microscopy, scanning electron microscopy (SEM), and energy dispersive spectroscopy (EDS). A simulation model was built to illustrate the possibility of liquid cavitation at the leaking region of the tube.

Jesús González et al. [3] Evaluated the retrofitting of industrial steam cracking furnace using CFD simulations. Their results showed that a reduction in the number of operative burners led to higher inhomogeneity in coil temperatures in the radiant section. And a reduction of 25% in crossover length led to a 2% increase in energy efficiency.

Yuan et al. [4] investigated analytical models for heat transfer in the tube bundle of the convection section in a steam cracking furnace. They developed a heat transfer analysis model for the tube bundle. Their study showed that convective heat transfer was significantly enhanced by fins in the tube bundles where the flue gas temperatures were too low to effectively heat the feedstock. Thus, the radiative heat transfer at the bottom of the convection chamber was much larger than the convective heat transfer; therefore, it could not be ignored in the heat transfer calculation.

Keshavarz et al. [5] modelled an industrial scale reaction furnace using computational fluid dynamics. From the obtained results, it can be found that sulfur dioxide was formed at the interface of air and acid gas and its rate of formation reached its maximum rate at the air swirling area.

Zheng et al. [6] numerically studied a distributed parameter model for a turbulent reactor in an ethylene cracking furnace based on continuous assessment of three-dimensional combustion. Their mathematical model was formulated for the prediction of heat flux and pipe temperature distributions considering a non-uniform distribution of superficial heat transfer and ethylene pyrolysis process. Their results showed that there are four sections in the distribution of heat flux in the turbulent reactor and the maximum pipe temperature is up to 1080 ℃. They believed that this distributed parameter model could be used as a guideline for cracking furnace operation as well as a tool for design.

Taweerojkulsri et al. [7] investigated the temperature control of EDC cracking furnaces. They modelled the EDC cracking process inside a furnace using a set of the ordinary differential equation (ODE), and two-dimensional partial differential equation (PDE). In other words, they modelled the heat transfer of coils inside the furnace, usually considered as radiative heat transfer, through two sets of ODE-PDE. For the sake of simplicity in this research, fluid flow was considered as plug flow, and the obtained results were compared with the results of a turbulent flow case along with the κ-ε model. They stated that the average velocity was the same in both cases, and the plug flow assumption could be considered for the simplicity of the model.

Heynderickx et al. [8], Oprins et al. [9,10], Stefanidis et al. [11,12], Coelho [13], and Habibi et al. [14] analyzed the velocity and temperature profiles at the radiation section of a cracking furnace, using numerical methods. They evaluated the influences of mesh type and radiation model on the numerical simulation of a combustion furnace. Furthermore, two other groups of researchers, Lan et al. [15], and Han et al. [16] simulated different cases of cracking furnaces through the CFD simulation software. They focused on the detailed investigation of the velocity

profile, temperature, and concentration fields inside the cracking furnaces. In another study, Liu et al. [17] improved and developed presented CFD models for cracking inside furnaces which led to the improvement in computational efficiency and performance. Also, Hu et al. [18,19] presented a binary method (dual method) for the simulation of pipes of the combustion chamber using CFD simulation in Coilsim1D software package.

Liu et al. [20], and Zhou and Yang [21] studied the convective heat transfer inside furnace coils and improved the existing results in this field through developing the available models using modelling. De Schepper et al. [22] added the terms of energy and mass source through volume fraction into the equations toward increase the numerical solution controllability and saving the computational time. Mahulkar et al. [23,24], and De Schepper [25] studied the numerical simulation of the cracking reaction of heavy feed pyrolysis. They offered some suggestions for the decrease of the coke thickness through the investigation and analysis of the results in this field. Furthermore, Mertinger et al. [26] studied the cause of corrosion of thermal pipes in the convection heat transfer section through ANSYS fluent software.

De Schepper et al. [27] simulated the exhaust gas from the stack and the gas inside heat exchanger tubes at the convective heat transfer section with the help of CFD. They simulated the heat transfer at only one constant heat flux in the convection section. Additionally, they considered negligible temperature variation in feed inside the vaporization section which this assumption can significantly affect the results of simulation and make an error in obtained results.

Pham et al. [28] presented a three-dimensional computational fluid (CFD) dynamics model with new permeability equations to study the release of gaseous gases in a four-zone low-temperature furnace (LTF) for carbon fiber carbonization. Four performance criteria (residence time, dead-volume ratio, temperature standard deviation, and tar formation area) were proposed to optimize the process.

Herce et al. [29] investigated the burner efficiency based on numerical (CFD) techniques and experimental measurements at the plant. To monitor burner efficiency, a new methodology based on CFD calculation of OH- and CH- radicals via reduced chemical kinetics, combined with industrial-scale experimental validation through flame spectroscopic measurements and UV CCD cameras, has been carried out.

Although several papers can be found on the simulation of thermal cracking furnaces, fewer papers were specifically devoted to the EDC thermal cracking. In this study, Two- and three-dimensional CFD simulations of an EDC thermal cracking furnace were compared. The influence of radiation flux on the coil surface was investigated as two separate cases: the constant heat flux on the whole coil surface, and the variable heat flux. Furthermore, the effects of the feed inlet temperature and mass flow rate on the EDC conversion, temperature, and mass fraction of the products were studied. The main advantage of this study is the comparison of the simulated results with the industrial data which can make the results of modelling to be more robust and applicable.

Research Methodology

Physical Model and Geometric Specifications

In this research, a vertical box-type cracking furnace was considered that schematically depicted in Fig. 1. This furnace is divided into three sections, i.e., vapor generator system (vaporization section), convection section, and cracking section. The first section is a vapor generator embedded in the furnace combustion gas path, on top of the convection section and under the furnace exhaust, and uses thermal energies of the exhaust gas for steam generation. In the second section of the furnace, preheated EDC at the pressure of about 26 bara (or 25

barg) enters the convection section and is heated up close to its boiling point about 210 ℃. Next, the hot EDC liquid comes out from the furnace and enters into the evaporator towards increasing the temperature through heat transfer by the exhaust gas of the cracking section. Finally, vaporized EDC enters the radiation section of the furnace and cracked at 280 ℃ and about 20.5 bara. The cracking conditions of the considered furnace will completely be described in the modelling section. Specifications of pipes such as size and material were reported in Table 1.
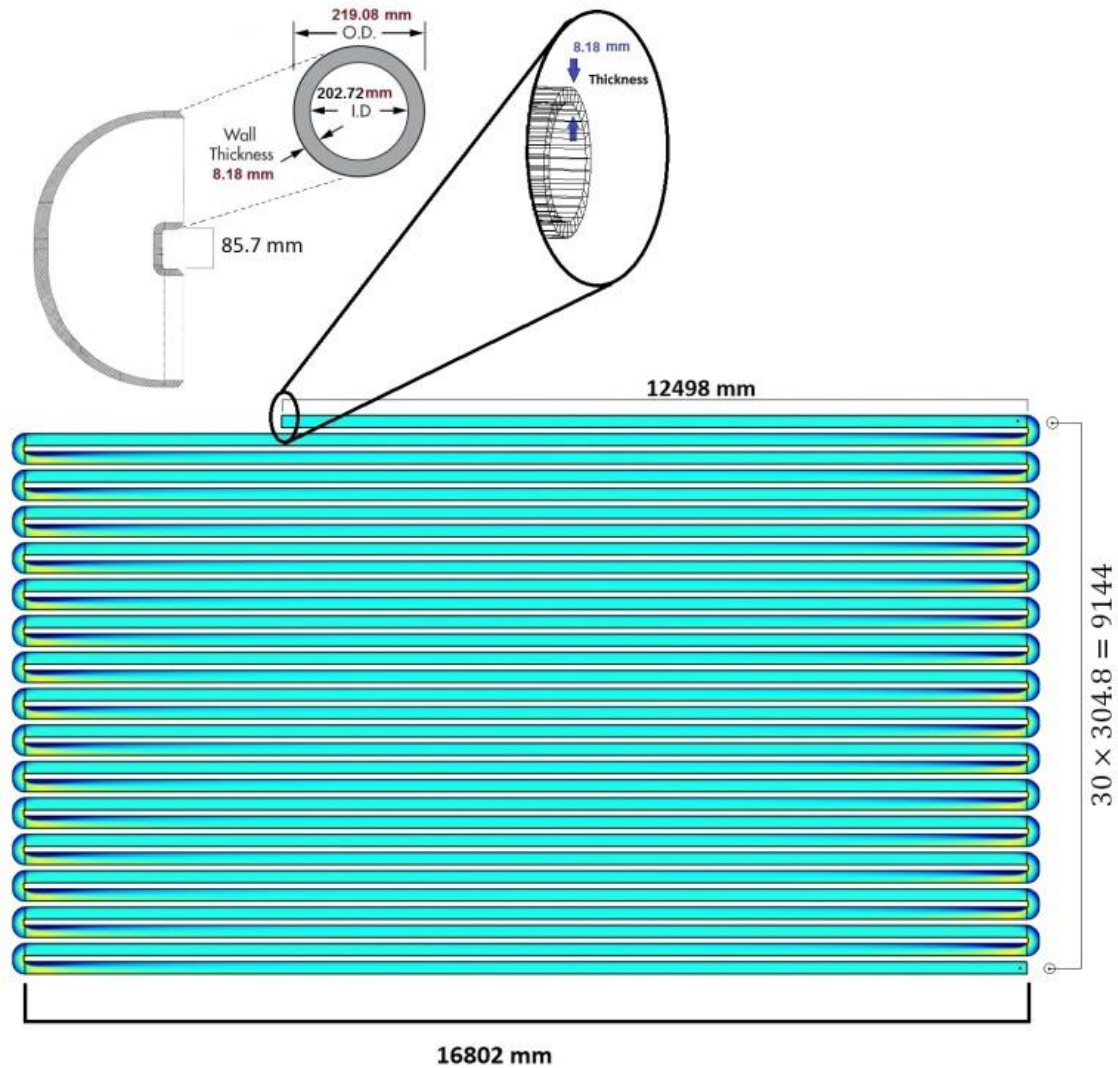

Fig. 1. Schematics of the 31 passes of the furnace radiation section

Table 1. Specifications of the coils

Quantity	Value
size	8"
material	Stainless Steel
type	ASTM A 312 TP347H
O.D. (mm)	219.08
Wall Thickness (mm)	8.18

EDC Cracking Equations

Momentum Transfer

To predict the velocity and pressure profile inside the coils, the continuity, and Navier- Stokes equations along with k-ε turbulence model were solved [30].

$$\nabla\left(\rho u\right)=0 \tag{1}$$

$$\rho\left(u.\nabla\right)u=\nabla.\left[-pI+\left(\mu+\mu_T\right)\left(\nabla u+\left(\nabla u\right)^T\right)-\frac{2}{3}\left(\mu+\mu_T\right)\left(\nabla u\right)I-\frac{2}{3}\rho kI\right]+F \tag{2}$$

The k-ε model is one of the turbulent flow models generally used for industrial applications. This model consists of a turbulence kinetic energy (k) and a rate of turbulence dissipation (ε) that introduces two additional transfer equations and two dependent variables. Also, the turbulence viscosity is defined as a variable for this model as Eq. 3 [30]:

$$\mu_T=\rho C_\mu\frac{k^2}{\varepsilon} \tag{3}$$

where C_μ is a constant parameter. The transfer equation for k is as Eq. 4:

$$\rho u.\nabla k=\nabla.\left(\left(\mu+\frac{\mu_T}{\sigma_k}\right)\nabla k\right)+P_k-\rho\varepsilon \tag{4}$$

and the production term is defined as Eq. 5:

$$P_k=\mu_T\left(\nabla u:\left(\nabla u+\left(\nabla u\right)^T\right)-\frac{2}{3}\left(\nabla.u\right)^2\right)-\frac{2}{3}\rho k\nabla.u \tag{5}$$

The transfer equation for the ε term is also written as Eq. 6:

$$\rho u.\nabla\varepsilon=\nabla.\left(\left(\mu+\frac{\mu_T}{\sigma_k}\right)\nabla\varepsilon\right)+C_{\varepsilon 1}\frac{\varepsilon}{k}P_k-C_{\varepsilon 2}\rho\frac{\varepsilon^2}{k} \tag{6}$$

The model constants in Eq. 4 and Eq. 6 are experimentally calculated, and their values for general applications are given in Table 2.

Table 2. The constants of turbulence model [30]

Constant	Value
C_μ	0.09
$C_{\varepsilon 1}$	1.44
$C_{\varepsilon 2}$	1.92
σ_k	1
σ_ε	1.3

Energy Transfer

In addition to the fluid flow equations, the heat transfer phenomenon also occurs in this heat exchanger. Additionally, there are some parameters such as viscosity in the fluid flow calculation which are temperature-dependent. In the model, the fluid dynamics and heat transfer equations are solved coupled together. The general heat transfer equation for the heat transfer of fluid inside the coils is expressed in Eq. 7 [30]:

$$\rho C_p\left(\frac{\partial T}{\partial t}+u.\nabla T\right)+\nabla.\left(q+q_r\right)=\alpha_pT\left(\frac{\partial p}{\partial t}+u.\nabla p\right)+\tau:\nabla u+Q \tag{7}$$

According to the steady-state simulation of EDC cracking, the influences of viscosity dissipation, as well as the work due to pressure changes, is neglected in Eq. 7 and it is therefore simplified to the following form:

$$\rho C_p u.\nabla T+\nabla.\left(q\right)=Q \tag{8}$$
$$q=-k\nabla T \tag{9}$$

where Q is the heat source. And in this study, Q is the amount of consumed heat by cracking reaction inside the coils. Eq. 10 shows the amount of heat consumption.

$$Q = R_{EDC} \times \Delta H_r \tag{10}$$

The rate in Eq. 8 is obtained by solving the k-ε turbulence model in fluid flow.

Mass Transfer

Eq. 11 is provided for describing the mass transfer of i species in the gas mixture in the general state. In this equation, w_i represents the mass fraction of i in the coil.

$$\frac{\partial}{\partial t}(\rho \omega_i) + \nabla.(\rho \omega_i u) = -\nabla.j_i + R_i \tag{11}$$

$$i = EDC, VCM, HCl$$

where ρ is the density of the gas mixture (kg/m^3), and u is the velocity field obtained from the momentum transfer section as the coupled variables. On the left side of Eq. 11, the first term corresponds to the accumulation of species in the coil, which is neglected in this study due to steady-state simulation. The second term on the left side of the equation describes the convection regarding u (m/s) direction. On the right side, the first term introduces the dispersion of species due to gas-phase diffusion, and the second term (R_i) is the reaction rate for each species in the process expressed as Eq. 12.

$$R_{EDC} = -k_0 e^{\frac{-E}{RT_g}} C_{EDC} \tag{12}$$

Kinetics of the Reactions

Vinyl chloride monomer (VCM) is a raw material for the production of polyvinyl chloride (PVC) which is commonly obtained from cracking of ethylene dichloride (EDC) at about 400-500 °C. In this process, hydrogen chloride (HCl) is considered as a side product. Generally, this reaction is considered as follow:

$$C_2H_4Cl_{2(g)} \rightarrow C_2H_3Cl_{(g)} + HCl_{(g)} \tag{13}$$

EDC   VCM   Hydrogen Chloride

Although, a radical chain reaction model developed by Schirmeister et al. [31], consists of 31 reactions and 24 compounds, where eight of the compounds are radicals, in this study a simplified reaction scheme including the main reaction is used as mentioned in Eq. 13. The model developed by Schirmeister et al. [31] is much more complex than the simplified reaction scheme used in this study. Although the simplified model cannot be used for extensive predictions of the byproducts, it is more convenient to be used for tuning the heat transfer model. The parameters of the reaction kinetics are summarized in Table 3.

Boundary Conditions

At the feed inlet, a constant velocity boundary condition corresponding to the mass flow rate as well as a constant concentration boundary condition corresponding to feed concentration was defined. Also, a constant temperature boundary condition was used for the heat transfer equation. All the boundary conditions are summarized in Table 4.

Table 3. Parameters used in the model to simulate EDC cracking

Name	Expression	Description
E	1.15×10^5 J/mol	Activation energy
ΔH	-70.7 kJ/mol	Heat of reaction
ε	0.8	Emissivity of tube skin
K_0	1.15×10^7 1/s	Kinetic constant
K_g	2.66×10^{-2} W/(m.K)	Thermal conductivity of gases in tube
M_{EDC}	98.96 g/mol	EDC molecular weight
μ_g	1.7×10^5 kg/(m.s)	Viscosity of cracked gases
ρ_g	83.425 kg/m^3	Cracked gas density
$C_{p,g}$	1455.7 J/kg.K	Average heat capacity of cracked gases
M_{HCl}	36.46094 g/mol	HCl molecular weight
M_{VC}	62.45 g/mol	VCM molecular weight
V_{in}	m/ ρ_g/(pi.(0.2109 [m])$^{2.4}$)	Inlet velocity
T_{amb}	600 °C	Ambient temperature
Re	$\rho_g.V_{in}\times0.2109$ [m]/ μ_g	Reynolds number
m	62308 kg/h	Mass flow rate
T_{in}	240 °C	Inlet temperature
Tb_1	850 °C	Bulk temperature, Zone 1
Tb_2	800 °C	Bulk temperature, Zone 2
Tb_3	750 °C	Bulk temperature, Zone 3
Tb_4	700 °C	Bulk temperature, Zone 4
Ts_1	400 °C	Surface temperature, Zone 1
Ts_2	420 °C	Surface temperature, Zone 2
Ts_3	440 °C	Surface temperature, Zone 3
Ts_4	450 °C	Surface temperature, Zone 4

Table 4. Summary of the applied boundary conditions in the simulation

Boundary	Differential equation	Boundary condition
Inlet	Momentum	$V=V_{in}$ P= 19 bar
	Mass transfer	$C_{EDC} = C_{EDC,0}$ $C_{VCM} = 0$ $C_{HCl} = 0$
	Heat transfer	$T= T_{in}$
outlet	Momentum	$P = 0$
	Mass transfer	C_{EDC} = convective flux C_{VCM} = convective flux C_{HCl} = convective flux
	Heat transfer	$n.q = 0$

A specific boundary condition is applied to the coil walls. N_i is the total mass transfer that is equal to the sum of diffusive and convective flux which is assumed to be zero on the wall of the coils. Furthermore, due to the turbulence of the flow inside the coils, the normal velocity on the surface is equal to zero, and the tangential velocity is represented as a relation. In the energy transfer equation, the constant radiative heat flux is defined on the walls.

On the walls:

Mass transfer

$$-n.N_i = 0$$
$$N_i = j_i + \rho u \omega_i \tag{14}$$
$$i = EDC, VCM, HCl$$

Momentum transfer

$$u.n = 0 \tag{15}$$

$$\left[-pI + (\mu + \mu_T)\left(\nabla u + (\nabla u)^T\right) - \frac{2}{3}(\mu + \mu_T)(\nabla.u)I - \frac{2}{3}\rho k I \right] n = -\rho \frac{u_\tau}{\delta_w^+} u_{\tan g} \tag{16}$$

$$u_{\tan g} = u - (u.n)n \tag{17}$$

Energy transfer

$$\nabla k.n = 0 \quad , \quad \varepsilon = \rho \frac{C_\mu k^2}{K_v \delta_w^+ \mu} \tag{18}$$

$$q = \sigma \times \varepsilon \left(T_b^{\ 4} - T^4\right) \tag{19}$$

After explaining the equations and boundary conditions, the parameters required to solve these equations were extracted from literature, and the operating conditions of the EDC cracking unit and were reported in Table 3.

Assumptions

For the numerical solution of the EDC cracking process and solving their PDEs, some assumptions are considered that are explained in the following.
- Gases are considered ideal gases.
- Physical properties are considered constant.
- The process is simulated in three and two-dimensions.
- A simplified reaction scheme is used. The cracking reaction is considered as a single-step reaction, and the side reactions are ignored.
- Radiation from furnace walls to the coil is defined as heat flux on coil walls.
- To consider the actual conditions in the simulation, the coil is divided into four sections based on the amount of received heat flux from the furnace; according to the furnace temperature at different sections.
- The friction of gas with the furnace walls and the pressure drop caused by it are neglected.
- Coke formation on the coil internal surfaces is neglected.

Meshing in CFD Modeling

In this modelling, the free triangular elements were used for meshing the geometry. The mesh distribution near the walls provides sufficient accuracy to solve the equations of the boundary layer near the solid-fluid interface. To increase the accuracy of the calculated values, the mesh number at the boundary layer region was increased. Also, to achieve sufficient accuracy at the boundary layer near the solid-fluid interface, a smaller mesh distribution near the walls was used which is illustrated in Fig. 2.

Results and Discussion

At the first step of this study, coil pass inside the furnace was simulated in three-dimensions and the obtained results were compared at similar operating conditions with equal length of a two-dimensional model. Due to a small difference between the results of the two-and three-dimensional models, and also reducing the simulation costs (time and quantity of the calculation), at the next steps, the simulation was performed in two-dimensions for the entire furnace (whole 31 passes). The optimal mesh was selected based on the EDC conversion along

the coil length. Then, two-dimensional simulation results are compared with industrial results towards confirming the validity of the simulation results. Consequently, the influence of flow rate, and the gas inlet temperature into the coil on EDC conversion, and the temperature distribution along the coil were investigated.
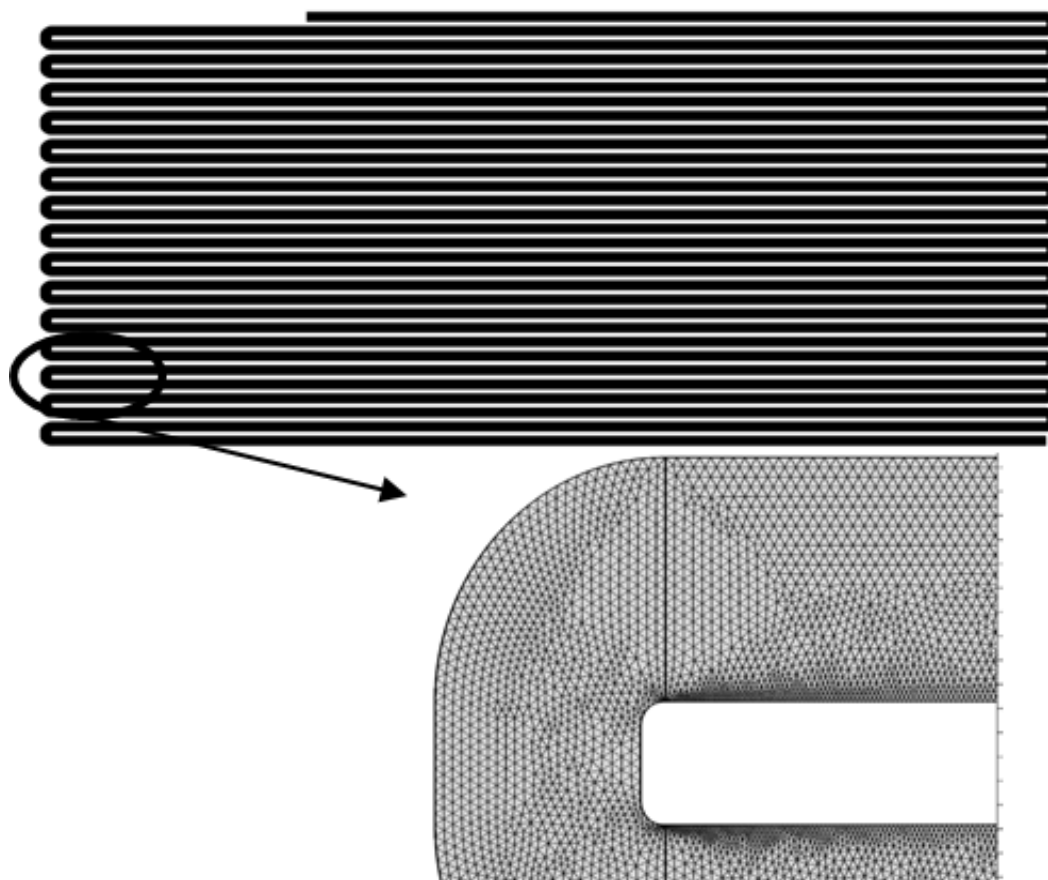

Fig. 2. Illustration of two-dimensional coil meshing inside the EDC cracking furnace

Three-Dimensional Simulation of One Pass

First of all, three-dimensional modelling of only one pass from the coil with 16 m long inside the furnace was performed. The inlet temperature in this section is 300 ℃, and the furnace temperature is 600 ℃. According to the endothermic nature of the cracking reaction, the heat required for this reaction was considered as the radiation on the surface of the coil pipes. Regarding the gas inlet flow rate, fluid flow inside the pipes was simulated as a turbulent flow. The concentration profiles of the reactant and the products are shown in Fig. 3. The EDC mass fraction at the inlet of the coil is equal to unity, and the product mass fractions (VCM and HCl) are assumed to be zero. As can be seen in Fig. 3, the EDC conversion increased along with the coil. On the other hand, more conversion occurred near the walls due to the applied heat flux on the coil wall, and the endothermic nature of the cracking reaction.

The mass flow rate or the inlet velocity to the coil is the most important parameter in the design and simulation of systems containing mass transfer and chemical reaction. The EDC residence time inside the coil decreases with increasing the inlet flow rate (velocity). And also the amount of absorbed heat by the fluid from the furnace environment decreases. Consequently, according to Fig. 4, it is observed that the EDC conversion along the three-dimensional simulated pass decreases from %4.29 to %2.65 with an increase in the inlet velocity from 4 m/s to 6.9 m/s. An increase in the inlet velocity of the fluid decreases the gas residence time inside the pipe, consequently, the EDC conversion decreases.
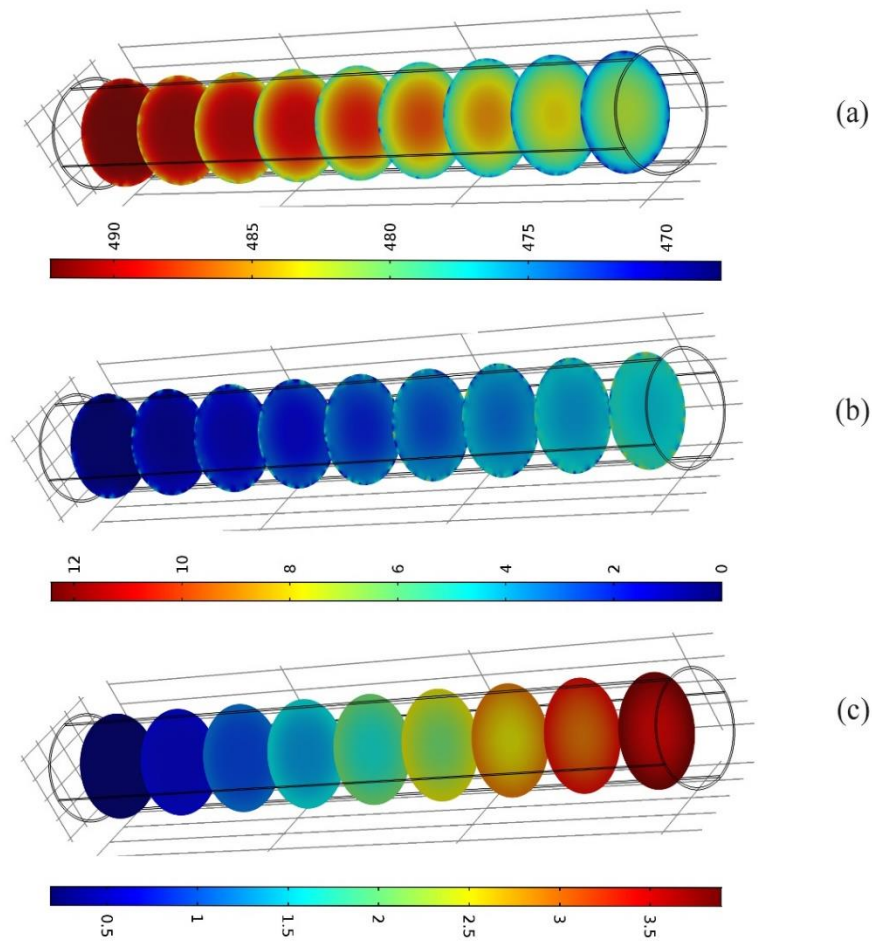
Fig. 3. Concentration distribution inside the first pass in the case of three-dimensional simulation:
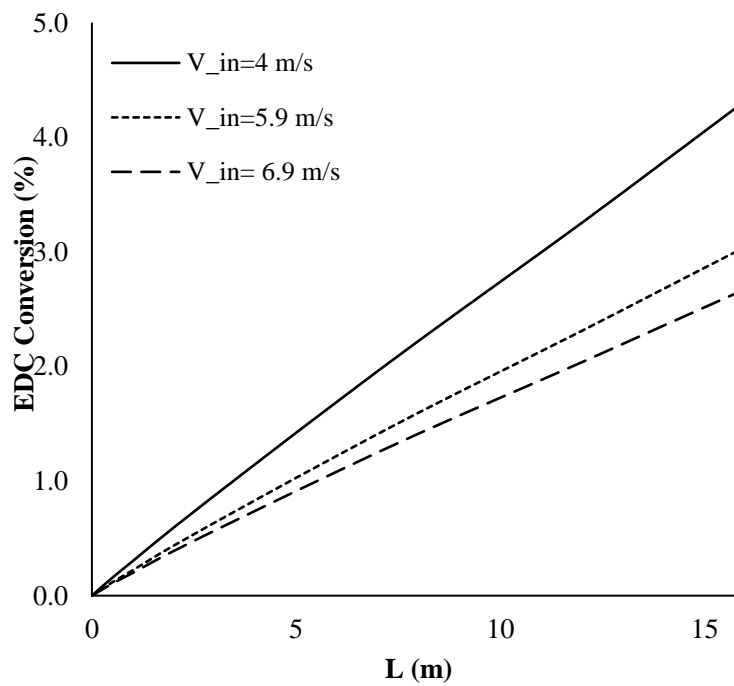(a) EDC, (b) HCl, (c) VCM (mol/m^3)

Fig. 4. The influence of inlet velocity on the EDC conversion at the first pass of the coil in the case of three-dimensional simulation

Fig. 5 shows an evaluation of the influence of the EDC inlet temperature on the coils in three cases of 300, 350, and 400 ℃ on the EDC conversion. As can be seen in Fig. 5, EDC conversion increases at the higher inlet temperature due to the endothermic nature of the cracking reaction. As shown in Fig. 5, increasing the inlet temperature from 300 to 400 ℃ increases the EDC conversion from %2.31 to %7.
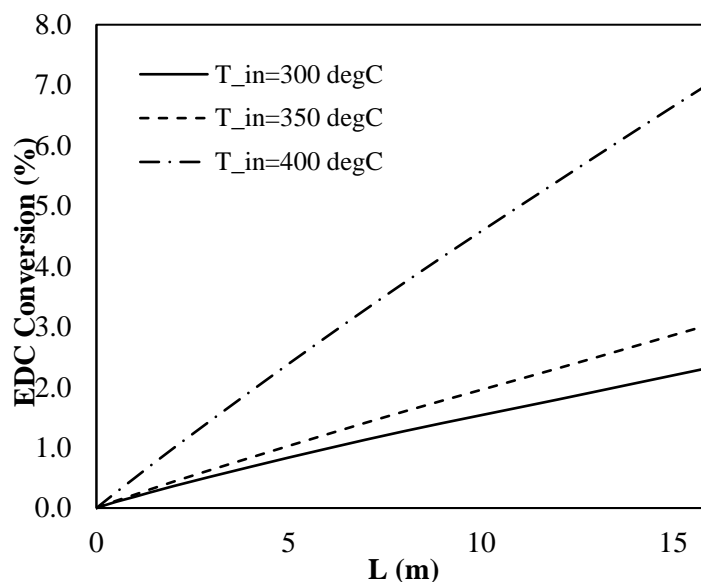

Fig. 5. Influence of the coil inlet temperature at the first pass of the coil in three-dimensional simulation

Another important parameter of this study is the inside temperature of the furnace. In this section, the furnace temperature was investigated in three cases of 500, 600, and 700 ℃. By increasing the furnace environment temperature, the amount of radiation and consequently, the heat flux on the coil walls increases which enhances the temperature of the fluid inside the coil and leads to an increase of the EDC cracking rate. The increase in EDC conversion along the first pass is shown in Fig. 6. The results show that, with increasing the temperature of the furnace environment from 500 to 700 ℃, the EDC conversion increases from %2.16 to %4.3.

Two-Dimensional Simulation

One of the main problems of a three-dimensional simulation of the coils inside the furnace is the large volume of computations due to simultaneous solving of momentum, turbulence, and mass transfer equations along with the chemical reactions and energy balance. For a better understanding of the cracking process inside the furnace, in the following, all passes of the coil inside the furnace were two-dimensionally simulated. For this purpose, before comparing the results with the available industrial data, first, two-and three-dimensional simulation results were compared for the first pass outlet in 16 m length. Results of both cases including the EDC conversion and outlet temperature are compared in Table 5. As can be seen, the difference between two-and three-dimensional simulations is small, and it is possible to simulate all passes in a two-dimensional simulation.

Mesh Independence

To evaluate the dependency of the results on the geometry meshing, the number of nodes and the element size was changed so that the results, particularly in term of EDC conversion along with the coil, are not dependent on the geometry meshing. The EDC conversion along with the coil as illustrated in Fig. 7 considering different mesh sizes.

As can be seen in Fig. 7 for element number 1,302,588, the difference in EDC conversion with that of 1,609,283 is less than 5%. Therefore, in this study, the element number of 1,302,588 was used.
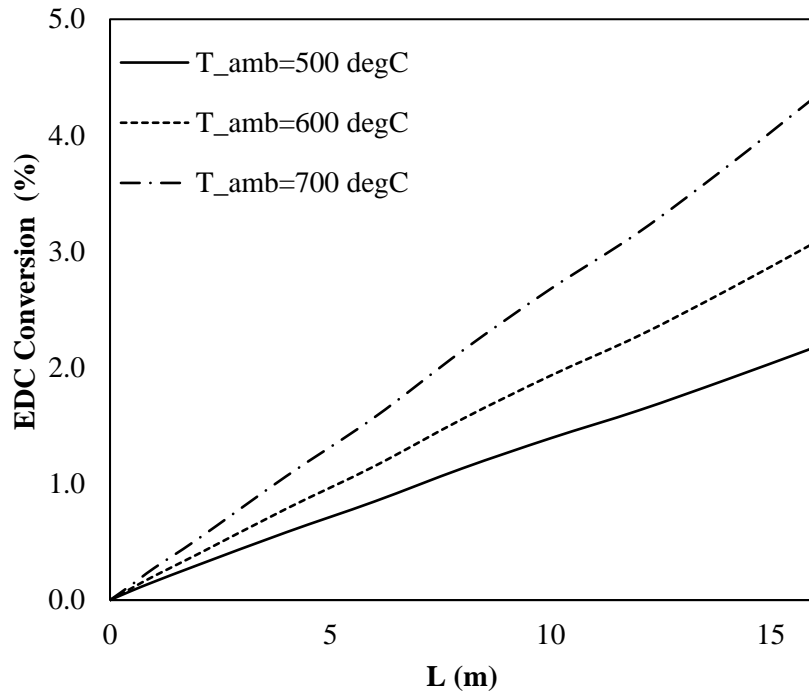

Fig. 6. Effect of furnace environment temperature on the EDC conversion at the first pass of the coil in three-dimensional simulation

Table 5. Comparison of the two and three-dimensional simulation results of the first pass

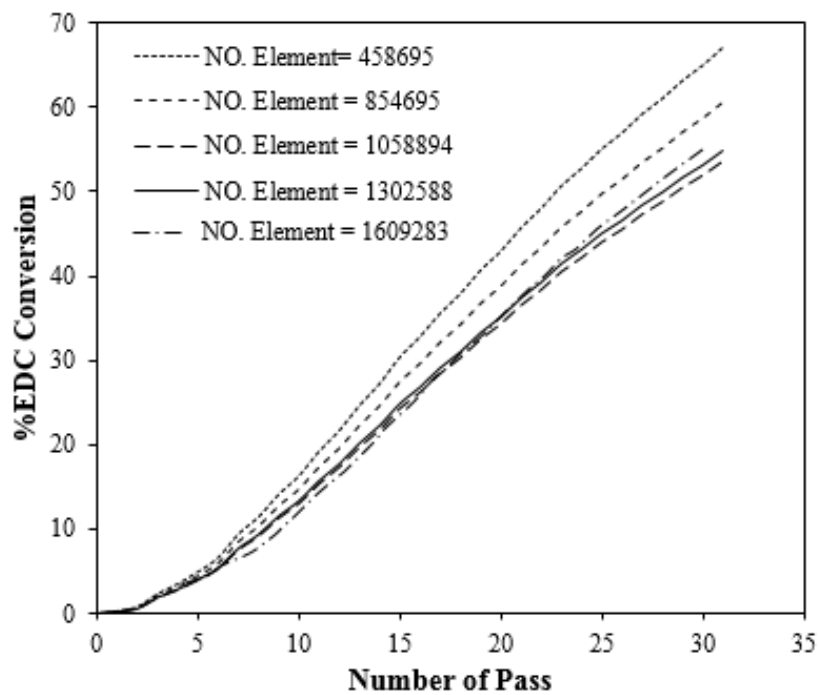|	2-dimensional	3-dimensional	Difference (%)
EDC conversion	2.056511	2.1155	2.78
Outlet temperature (℃)	355.343	356.2134	0.25

Fig. 7. Influence of mesh size on EDC conversion along the coil

Also, the characteristics of the chosen mesh in COMSOL Multiphysics software are shown in Table 6. As observed, the average quality of the chosen mesh is about 99%. Therefore, this number of elements was used for the evaluation of other results and operational conditions.

Table 6. Properties and characteristics of the final meshing used in this project for the two-dimensional geometry

Complete Mesh		Domain element Statistics	
Mesh vertices	689,167	Number of elements	1,302,588
Element Type	All Element	Minimum element quality	0.5021
Triangular elements	1,302,588	Average element quality	0.9876
Edge elements	76,884	Element area ratio	0.006118
Vertex elements	304	Mesh area	1.072×10^8 mm^2
-	-	Maximum growth rate	2.448
-	-	Average growth rate	1.047

Validation and Verification of the Results

Although a lot of results were obtained through modelling some of them can be compared with the industrial data results due to limitations of monitoring and measurement on an industrial scale. For this purpose, the EDC conversion and the concentration of products (VCM, HCl) at the coil outlet, the pressure drop of the coil, and also the fluid outlet temperature of the coil in industrial and simulated cases and their deviations are reported in Table 7.

Table 7. Comparison of the results of simulation with the results of industrial data

	Simulation	Industrial	Deviation (%)
EDC conversion	54.94	54.44	0.91
Outlet temperature (K)	687.75	743.15	7.45
Mass fraction of EDC in outlet	45.05	43.38	3.85
Mass fraction of VCM in outlet	29.94	32.80	8.72
Mass fraction of HCl in outlet	25.00	19.04	23.84
Total pressure drop of the coil	0.6	1.02	41.18

As observed, the deviation of EDC conversion, and also the mass fraction of EDC in the coil outlet is very small between the simulation results and industrial data. The coil outlet temperature in the simulation results is less than the results of industrial data. This deviation can be due to the side reactions and coke formation inside the furnace which were neglected in the simulation. Additionally, it should be noted that the radiation of gas inside the coils was ignored in the simulation, and the heat only transferred through heat flux on the wall of the coils. Despite this, it is observed that the simulation results are in reasonable agreement with the industrial results.

On the other hand, the mass fraction of HCl in the simulation is moderately greater than that in industrial data. It is also shown in Table 7, that the total mass fraction of the three main components (EDC, VCM, and HCl) according to the industrial data is about %95. As the chemical analysis of the industrial products shows, the remaining %5 contains some chlorinated compounds which are the products of the side reactions ignored in this study. So, this deviation for HCl mass fraction is strongly related to the side reactions. The total pressure drop along the pass was less than that of the industrial data. It is mainly because coke formation was not considered in this study. Coke not only reduces the flow passage and increases the pressure drop but also increases the roughness of the internal surface of the coil which can duly increase the pressure drop.

Velocity and Pressure Inside the Coil in 2-D Simulation

The distribution of velocity and pressure in fluid flow systems is important. To obtain the velocity and pressure distribution inside the coil of the thermal cracking furnace, the Navier-Stokes equations along with k-ε turbulence equations were solved as coupled equations.

According to the industrial conditions, the gas inlet flow rate to the coil was considered as 62308 kg/h. According to the gas flow rate, the gas inlet velocity to the coil was about 6 m/s, and due to the compressibility of the gases and the pressure drop caused by the elbows, the velocity increases in the angular regions and returns to the former value again along the straight sections of the coil. The inlet pressure was 19.5 barg, and the total pressure drop along the passes was calculated as 0.6 bar which is in good accordance with the industrial data.

Effect of Heat Flux on the Walls of the Coil

To simulate the thermal cracking of the EDC cracking furnace, the energy equations are solved only for the coil inside the furnace. The connection of the coil to the furnace environment and burners is considered by the heat flux boundary conditions on coil walls. So that, it is shown as follows [30]:

$$q^* = \alpha\sigma\left(T_f^4 - T^4\right) \tag{20}$$

where α is the absorption coefficient of the coil that is equal to 0.85, and σ is the Stefan-Boltzmann coefficient. Also, T_f is the furnace temperature, and T is the temperature of the coil surface.

Determining the ambient temperature regarding the location of the burners inside the furnace is one of the basic difficulties in simulating the cracking process. In this regard, the furnace was divided into four sections through industrial measurements of the furnace temperature at different times and conditions, and averaging them. The temperatures of these four sections from up to down are 850, 800, 750, 700 °C, respectively. Furthermore, the temperatures of the coil surface in the four sections are considered to be 400, 420, 440, and 450 °C, respectively according to successive measurements in the cracking unit. Also, simulation of all passes has been carried out step by step regarding the available data along with various assumptions, which are briefly referred to in the following.

The First Case

In this case, the inlet temperature is considered to be 240 °C, which is the closest temperature to the industrial value regarding successive measurements in the cracking unit. Also, the temperature of the four assumed sections in the furnace from up to down are 850, 800, 750, 700 °C respectively. In this case, the thermal boundary condition on the walls is also considered as a constant heat flux. The heat flux in different sections in the first case is provided in Table 8.

Table 8. Heat fluxes at the four sections in the first case of the 2-D simulation

Section number	1	2	3	4
Heat flux (kW/m^2)	66.797	52.796	40.349	30.044

The EDC conversion with these conditions is equal to 52.89%, and the outlet temperature of the coil inside the furnace is 378.99 °C, which greatly differs from the industrial data. Considering the modelling results of the first case, it was found that initially, the fluid enters the coil at 240 °C, and since the cracking reaction occurs at the temperatures above 300 °C the gas temperature increases in the initial passes, and when it is reached the required cracking temperature, the reaction begins. So, in the initial passes, no reaction occurred due to the low inlet temperature. In this case, the outlet temperature was obtained at 379 °C. Also, the inlet and outlet EDC mass fractions were 1 and 0.47134. Also, the produced VCM and HCl mass fraction at the outlet of the coil were calculated 0.28629 and 0.24237, respectively.

The Second Case

In this case, the inlet temperature was considered to be 240 ℃, and the temperature of the four assumed sections in the furnace from up to down was considered to be 850, 800, 750, and 700 ℃, respectively. The thermal boundary condition is considered as radiation on the walls. In this case, all conditions were similar to the previous one, and the only difference is the variable heat flux boundary condition on the walls. In variable heat flux boundary conditions, the coil surface temperature is not divided into four sections and is not equal to a constant value. The surface temperature for the substitution in the Eq. 20 is a variable and should be obtained from the energy balance equation. In this case, the calculated heat flux on the coil walls is shown in Fig. 8, for two different mass flow rates. At the entrance, due to low coil temperature and the presence of fluid with a lower temperature inside it, the heat flux is higher and decreases along with the passes. This reduction in heat flux occurred stepwise which is due to the predefined ambient temperatures of the furnace. In this case, EDC conversion and the outlet temperature was obtained equal to 55% and 414.60 ℃, respectively. In the following, some of the results obtained from this case are shown. The mass fraction of VCM and HCl at the outlet of the radiation section is 0.30 and 0.25, respectively. The second case (considering the variable heat flux boundary condition) gives better results in comparison with the industrial data.
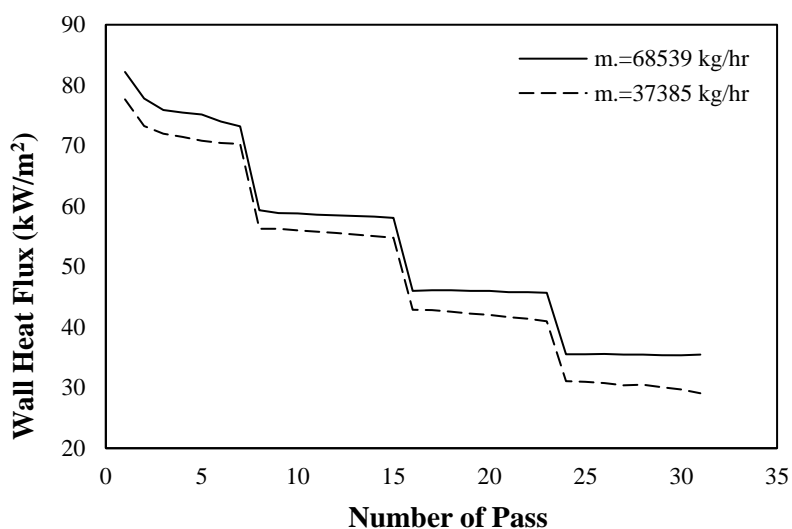

Fig. 8. Variable heat flux condition along different coil passes inside the furnace for the second case of simulation

As seen in the previous sections, the inlet temperature of the cracking furnace is one of the most important parameters in the EDC cracking process. The higher inlet temperature can lower the furnace heat duty for a specific conversion, or it can increase the cracking conversion of the EDC at a constant heat duty. Fig. 9 shows the effect of feed inlet temperature on EDC conversion for the second case of simulation at three different inlet temperatures of 240, 290, and 350 ℃. As shown in Fig. 9 by increasing the inlet temperature, the EDC cracking conversion increases in all passes.

The mass flow rate or inlet velocity is another important parameter in the systems that affects the mass transfer and chemical reactions. In this section, the mass flow rate was varied so that to be 60, 80, 100, and %110 of the total capacity. As mentioned, the EDC cracking process is endothermic and receives the required heat from the furnace through the defined heat flux on the coil surfaces. Therefore, decreasing the inlet mass flow rate increases the residence time in the coil inside the furnace, and also the amount of absorbed heat through the radiation. It increases the amount of cracking conversion. Fig. 10 shows the effect of inlet flow rate on the cracking conversion of EDC in the outlet of pass number 31. It is observed that the decrease in the flow rate significantly increases the amount of conversion.
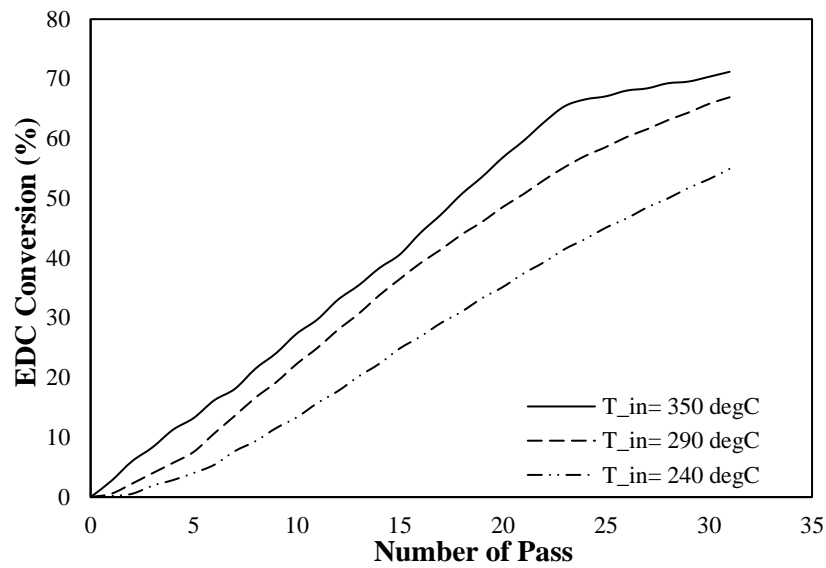
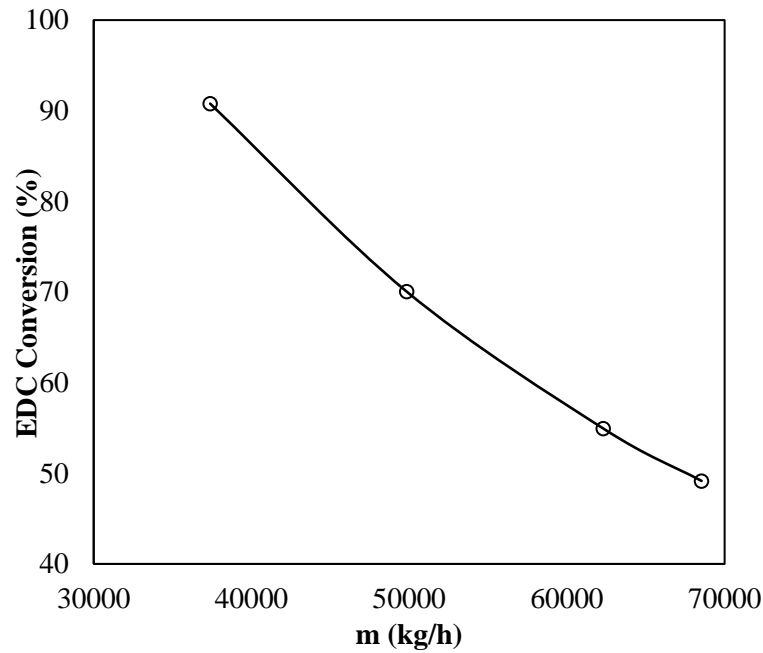**Fig. 9.** Effect of the feed inlet temperature on the cracking conversion of EDC

Fig. 10. Influence of inlet flow rate on EDC cracking conversion

HCl and VCM are the two main products of the cracking process. The mass fractions of these gases are given at different flow rates along with the passes in Figs. 11 and 12. As can be seen, the mass fractions of these gases also increase with increasing the residence time of the reactants inside the coil along with all passes.

Variation of the feed mass flow rate, as well as its effect on the mass fraction and cracking conversion, can significantly affect the temperature distribution inside the coil, and as a result, the outlet temperature of the coils. In other words, it can be argued that the increase in temperature caused by the flow rate reduction leads to an increase in cracking conversion in the coils. Therefore, it can be concluded that flow rate reduction in addition to increasing the residence time and conversion of the chemical reaction, increases the temperature inside the coil. Figs. 13 and 14 show the effect of the inlet flow rate on the outlet temperature of the coil, and the temperature of the gas along with the coil, respectively.
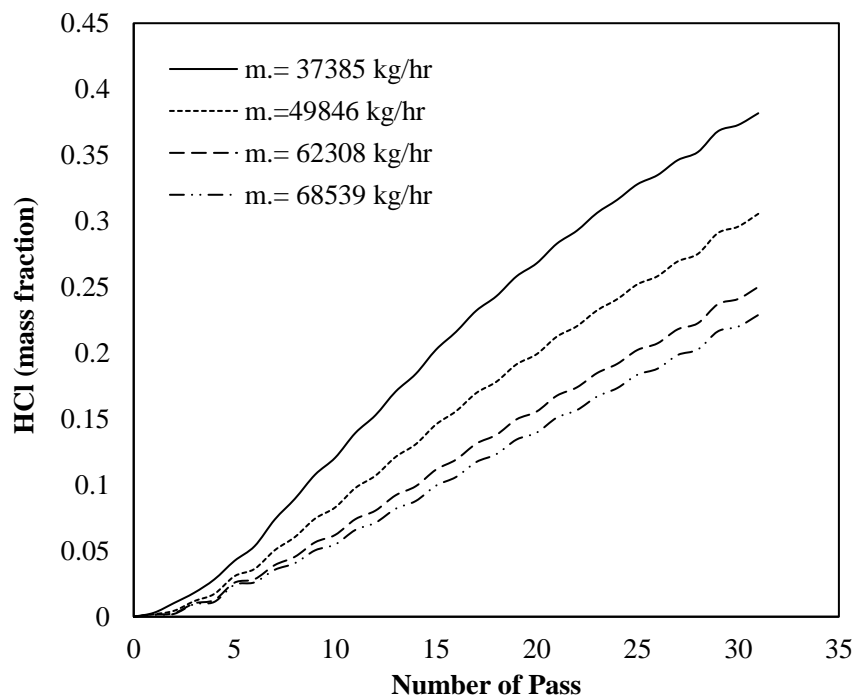
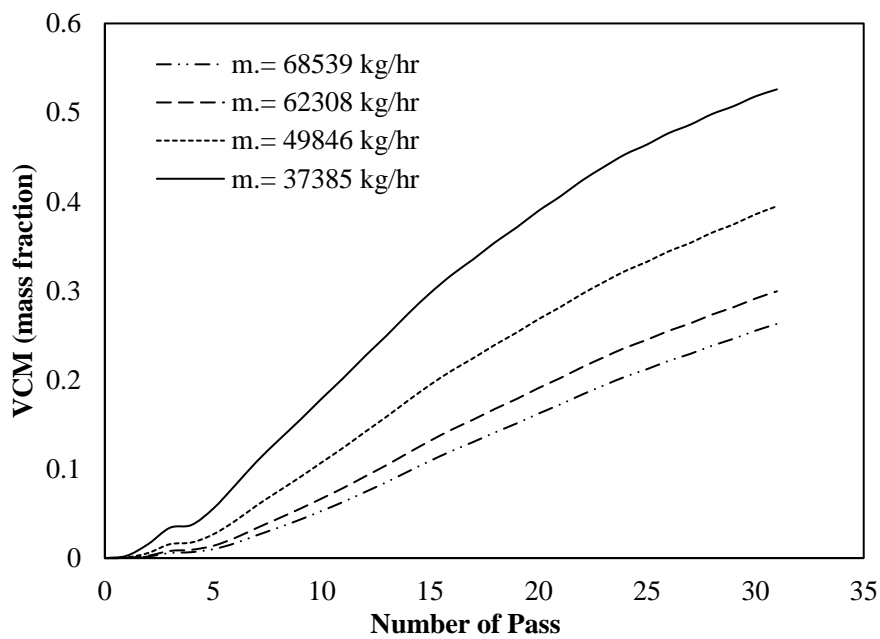**Fig. 11.** Influence of inlet flow rate on the HCl mass fraction along the passes

Fig. 12. Influence of gas inlet flow rate on the VCM mass fraction along the passes
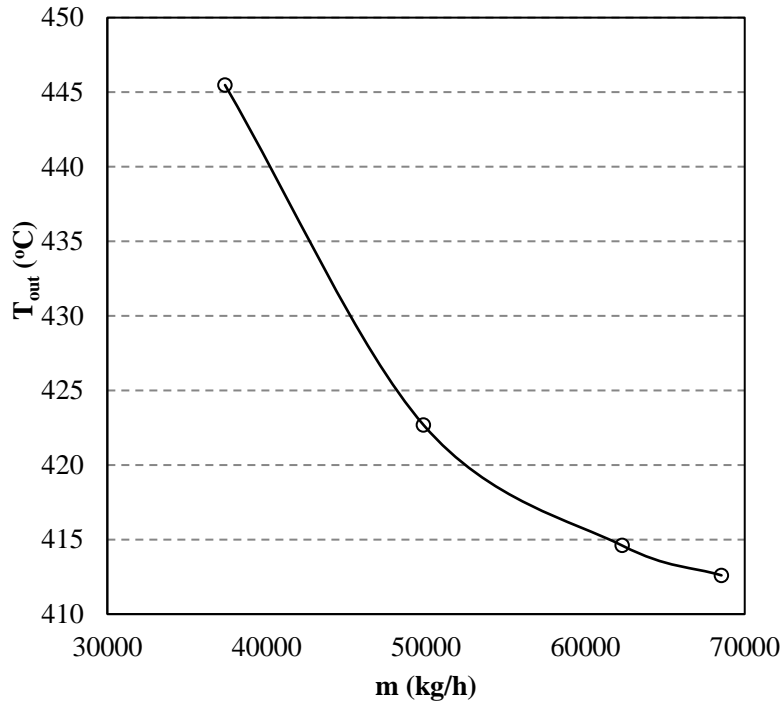
Fig. 13. Influence of inlet flow rate on the outlet temperature of pass number 31
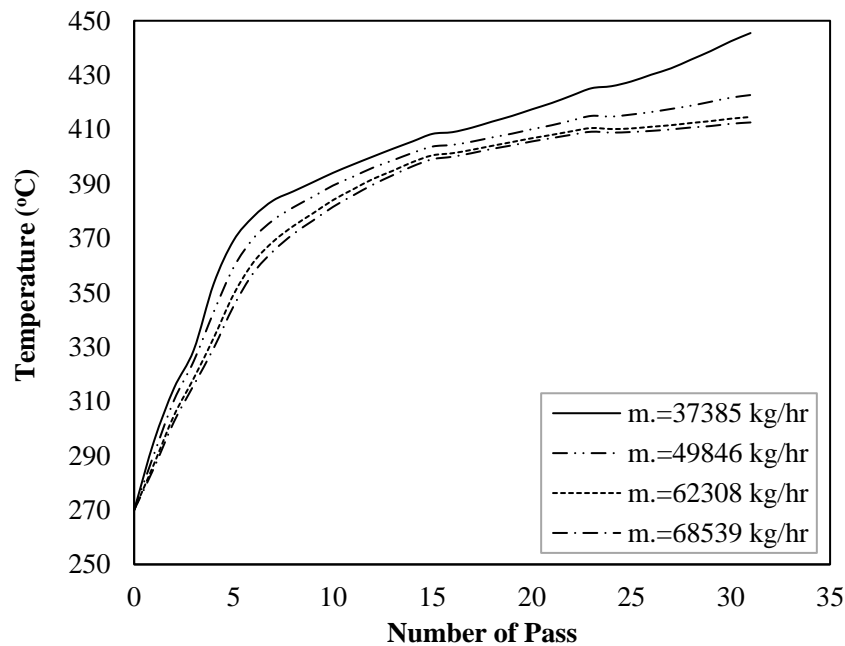

Fig. 14. Influence of inlet flow rate on the temperature distribution along the passes

Conclusion

In this study, the numerical analysis of the EDC cracking reaction inside the furnace using CFD with the finite element method was investigated. For this purpose, the Navier-Stokes equations along with turbulence equations, mass transfer equations with cracking reaction, and energy balance with radiation boundary condition are solved according to industrial conditions in the petrochemical unit. The main results showed that:

a) Two- and three-dimensional simulations of one pass were conducted. Comparing their results showed that less than 3 % deviation existed between the results of 2D and 3D. Thus, it was concluded that two-dimensional modelling is economically superior.

b) The influence of radiation flux on the coil surface was investigated in two separate cases. In the first case, constant heat flux was considered for the four sections of the coil surface, and in the second case, it was considered as a function of the temperature of the coil surface. The investigations showed that due to temperature changes along with the coil, considering the variable heat flux provided better results with respect to the industrial data.

c) Increasing the inlet temperature led to an increase in the EDC conversion due to the endothermic nature of the reaction.

d) The reduction in the feed mass flow rate increased the residence time, and as a result, it was led to a significant increase in the conversion, temperature, and mass fraction of the products.

List of symbols

E	Activation energy (J/mol)
ΔH	Heat of reaction (kJ/mol)
ε	Dissipation rate of turbulent kinetic energy (m^2/s^3)
K_0	Kinetic constant (1/s)
Kg	Thermal conductivity of gases in tube (W/m.K)
M_{EDC}	EDC molecular weight (g/mol)
μ_g	Viscosity of cracked gases (Pa.s)
j_i	Diffusion flux of species i
k	Turbulent kinetic energy (m^2/s^2)
ρ	Density (kg/m^3)
F	Volume force vector (N/m^3)
q	Heat flux (W/m^2)
μ_T	Turbulent Viscosity (Pa s)
Q	Heat sources (W/m^3)
ω_i	Mass fraction of species i (Eq. 11)
u	Velocity vector (m/s)
Ri	Reaction rate for each existing species
T_{in}	Fluid inlet temperature to the furnace (°C)
Vin	Fluid inlet velocity to the furnace (m/s)
P	Pressure (Pa)
α	Coil absorption coefficient
σ	Stefan-Boltzmann constant (5.67×10^{-8} W/m^2K^4)
C_i	Component concentration (i=EDC, VCM, HCl)
Ep	Turbulent dissipation rate
RANS	Reynolds Averaged Navier-Stokes
Ni	Total flux in mass transfer
T	Coil surface temperature (°C) (Eq. 14)
T_f	Furnace temperature (°C)

References

[1] Hu G, Yuan B, Zhang L, Li J, Du W, Qian F. Coupled simulation of convection section with dual stage steam feed mixing of an industrial ethylene cracking furnace. Chemical Engineering Journal. 2016 Feb 15;286:436-46.

[2]   Li W, Lv Y, Sun Z, Yu W. Cause analysis of corrosion leakage in convection section of ethylene cracking furnace. Engineering Failure Analysis. 2020 Mar 4:104488.

[3]   Rebordinos JG, Herce C, González-Espinosa A, Gil M, Cortés C, Brunet F, Ferré L, Arias A. Evaluation of retrofitting of an industrial steam cracking furnace by means of CFD simulations. Applied Thermal Engineering. 2019 Nov 5;162:114206.

[4]   Yuan B, Zhang Y, Hu G, Zhong W, Qian F. Analytical models for heat transfer in the tube bundle of convection section in a steam cracking furnace. Applied Thermal Engineering. 2019 Dec 25;163:113947.

[5]   Keshavarz E, Toghraie D, Haratian M. Modeling industrial scale reaction furnace using computational fluid dynamics: a case study in Ilam gas treating plant. Applied Thermal Engineering. 2017 Aug 1;123:277-89.

[6]   Zheng S, Zhang X, Qi C, Zhou H. Modeling of heat transfer and pyrolysis reactions in ethylene cracking furnace based on 3-D combustion monitoring. International Journal of Thermal Sciences. 2015 Aug 1;94:28-36.

[7]   Taweerojkulsri Ch, Panjapornpon Ch. Temperature Control of EDC Thermal Cracking Furnace with a Coupled ODE and 2D-PDEs Model. Chem. Eng. Sci. 2014; 31: 516–527.

[8]   Heynderickx GJ, Oprins AJ, Marin GB, Dick E. Three-dimensional flow patterns in cracking furnaces with long-flame burners. AIChE journal. 2001 Feb;47(2):388-400.

[9]   Oprins AJ, Heynderickx GJ, Marin GB. Three-dimensional asymmetric flow and temperature fields in cracking furnaces. Industrial & engineering chemistry research. 2001 Nov 14;40(23):5087-94.

[10] Oprins AJ, Heynderickx GJ. Calculation of three-dimensional flow and pressure fields in cracking furnaces. Chemical engineering science. 2003 Nov 1;58(21):4883-93.

[11] Stefanidis GD, Heynderickx GJ, Marin GB. Development of reduced combustion mechanisms for premixed flame modeling in steam cracking furnaces with emphasis on NO emission. Energy & fuels. 2006 Jan 18;20(1):103-13.

[12] Stefanidis GD, Merci B, Heynderickx GJ, Marin GB. CFD simulations of steam cracking furnaces using detailed combustion mechanisms. Computers & chemical engineering. 2006 Feb 15;30(4):635-49.

[13] Coelho PJ. Numerical simulation of radiative heat transfer from non-gray gases in three-dimensional enclosures. Journal of Quantitative Spectroscopy and Radiative Transfer. 2002 Aug 1;74(3):307-28.

[14] Habibi A, Merci B, Heynderickx GJ. Impact of radiation models in CFD simulations of steam cracking furnaces. Computers & Chemical Engineering. 2007 Nov 1;31(11):1389-406.

[15] Lan X, Gao J, Xu C, Zhang H. Numerical simulation of transfer and reaction processes in ethylene furnaces. Chemical Engineering Research and Design. 2007 Jan 1;85(12):1565-79.

[16] Han YL, Xiao R, Zhang MY. Combustion and pyrolysis reactions in a naphtha cracking furnace. Chemical Engineering & Technology: Industrial Chemistry-Plant Equipment-Process Engineering-Biotechnology. 2007 Jan;30(1):112-20.

[17] LIU S, WANG H, QIAN F, HU G. Coupled simulation of combustion with heat transfer and cracking reaction in SL-Ⅱ industrial ethylene pyrolyzer. CIESC Journal. 2011;62(5):1308-17.

[18] Hu G, Wang H, Qian F, Van Geem KM, Schietekat CM, Marin GB. Coupled simulation of an industrial naphtha cracking furnace equipped with long-flame and radiation burners. Computers & chemical engineering. 2012 Mar 5;38:24-34.

[19] Hu G, Schietekat CM, Zhang Y, Qian F, Heynderickx G, Van Geem KM, Marin GB. Impact of radiation models in coupled simulations of steam cracking furnaces and reactors. Industrial & Engineering Chemistry Research. 2015 Mar 11;54(9):2453-65.

[20] Liu JJ, Guo Y, Zhang LJ. Process simulation of the convection section of cracking furnace based on Asepen Plus user model. Tianjin Chem. Ind.. 2009;23:25-9.

[21] Zhou Y, Yang DZ. Simulation and optimum design for convection section of ethylene cracking furnace. Chemical Engineering (China). 2010;9.

[22] De Schepper SC, Heynderickx GJ, Marin GB. Modeling the evaporation of a hydrocarbon feedstock in the convection section of a steam cracker. Computers & Chemical Engineering. 2009 Jan 13;33(1):122-32.

[23] Mahulkar AV, Heynderickx GJ, Marin GB, Varbanov P, Lam H, Klemes J, Pierucci S. Simulation of coking in convection section of steam cracker. Chemical Engineering. 2012;29: 1375–1380.

[24] Mahulkar AV, Heynderickx GJ, Marin GB. Simulation of the coking phenomenon in the superheater of a steam cracker. Chemical Engineering Science. 2014 May 3;110:31-43.

[25] De Schepper SC, Heynderickx GJ, Marin GB. Modeling the coke formation in the convection section tubes of a steam cracker. Industrial & engineering chemistry research. 2010 Jun 16;49(12):5752-64.

[26] Mertinger V, Benke M, Szabó S, Bánhidi O, Bollo B, Kovács Á. Examination of a failure detected in the convection zone of a cracking furnace. Engineering Failure Analysis. 2011 Oct 1;18(7):1675-82.

[27] De Schepper SC, Heynderickx GJ, Marin GB. Coupled simulation of the flue gas and process gas side of a steam cracker convection section. AIChE journal. 2009 Nov;55(11):2773-87.

[28] Pham HH, Lim YI, Ngo SI, Bang YH. Computational fluid dynamics and tar formation in a low-temperature carbonization furnace for the production of carbon fibers. Journal of Industrial and Engineering Chemistry. 2019 May 25;73:286-96.

[29] Herce C, González-Espinosa A, Gil A, Cortés C, González-Rebordinos J, Guégués T, Gil M, Ferré L, Brunet F, Arias A. Combustion monitoring in an industrial cracking furnace based on combined CFD and optical techniques. Fuel. 2020 Nov 15;280:118502.

[30] Bird RB, Stewart WE, Lightfoot EN. Transport Phenomena. 2nd ed, John Wiley & Sons, 2007.

[31] Schirmeister R, Kahsnitz J, Träger M. Influence of EDC cracking severity on the marginal costs of vinyl chloride production. Industrial & engineering chemistry research. 2009 Mar 18;48(6):2801-9.